

Optimization Design of Disc Spring for Hydraulic Oscillator

Xinyuan Wu *, Junchi Lin

Mechanical Engineering College, Sichuan University of Science & Engineering, 644005 Yibin, China

* Corresponding author

Abstract: During drilling, hydraulic oscillators are commonly used to reduce the friction and resistance of the drill string. However, the disc springs in the oscillators short section can easily fail with increased service time. In this study, our aim was to improve the performance of the disc springs used in the oscillators short section by optimizing their design through response surface methodology. Using numerical and simulation techniques, we analyzed the mechanical properties and lifespan of the disc springs. We determined the optimal direction for the disc springs geometric structure using national standard algorithms. We established a parameterized model with thickness t and inner cone height h_0 as design variables and aimed to minimize stress, directed deformation, and maximize durability. As a result, we obtained the optimal structural parameters under the design conditions. The optimized disc spring reduced the maximum stress by 45.9%, with directed deformation accounting for 35.8% of the working stroke and achieving a minimum fatigue life of 154 hours. The use of the optimized disc spring improved the service time of the hydraulic oscillator, providing valuable insights for the optimization of disc springs in hydraulic oscillators.

Keywords: Disc springs; Finite elements; Fatigue analysis; Response surface; Parameter optimization.

1. Introduction

With the development of oil exploration technology, horizontal wells and high-displacement wells are becoming more and more common in order to increase oil and gas production. Due to the complex trajectory of such wells, drilling friction occurs between the drill string and the wellbore during sliding drilling, resulting in drilling costs far exceeding expectations [1,2] and seriously affecting the transmission of drilling pressure. Scholars at home and abroad have developed a hydraulic oscillator to address the friction reduction problem. By converting the hydraulic energy of the drilling fluid into mechanical energy, the tool produces periodic vibrations, effectively reducing the frictional resistance between the drill string and the wellbore [3-6]. The short section of the oscillator, as one of its components, relies on its core component, the disc spring assembly, to bear the alternating load and achieve periodic storage and release of energy. The parameter performance of the disc spring assembly directly affects the friction reduction efficiency of the tool. Most of the literature on disc spring assemblies used in the petroleum industry is based on standard series, and most of the non-standard disc springs are designed based on experience. This paper analyzes the existing small diameter ratio disc springs and optimizes the key structural parameters of the disc springs through the response surface method, improving their performance.

2. Hydraulic oscillator and disc spring geometric structure

(1) Principle of Hydraulic Oscillator

As shown in Figure 1, the hydraulic oscillator mainly consists of the pulse section and the oscillation section. When the drilling fluid flows through the pulse section, the sealing cavity produces unbalanced hydraulic pressure, driving the internal spool valve 7 to follow the rotor 6 to perform planetary motion around the fixed valve 8 surface of the stator 5

5, causing periodic changes in the flow area to generate periodic pulse pressure. The pulse pressure acts on the piston 3 to push the oscillation core axis 1, thereby driving the drill string to move axially, and at the same time, the disc spring assembly 2 stores energy. When the pulse pressure is less than the rebound force of the disc spring, the disc spring assembly releases energy to achieve periodic oscillation, changes the frictional state between the drill string and the wellbore, and enables the drill bit to obtain sufficient drilling pressure, thereby improving the drilling speed.

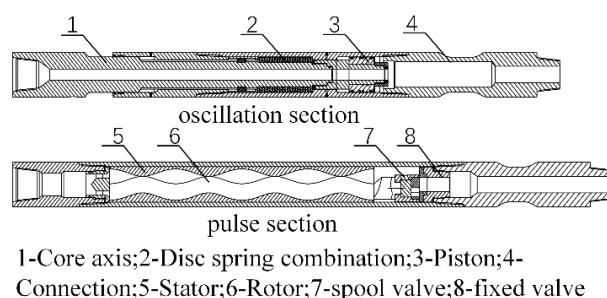


Fig. 1 Hydraulic oscillator structure diagram

(2) Structure Parameters of the Disc Spring

Disc springs have the advantages of small geometric structure, strong bearing capacity, and large deformation range. Generally, they often operate under small deformation conditions [7]. Figure 2 shows a two-dimensional schematic diagram of a non-standard disc spring used in a hydraulic oscillator, which has the same shape as the disc spring in the National Standard of the Peoples Republic of China GB/T 1972-2005 but has different structural dimensions (see Table 1). In Figure 2, D_i is the inner diameter of the disc spring, D_e is the outer diameter of the disc spring, H_0 is the free height of the disc spring, h_0 is the free height of the disc spring cone, and t is the thickness of the disc spring.

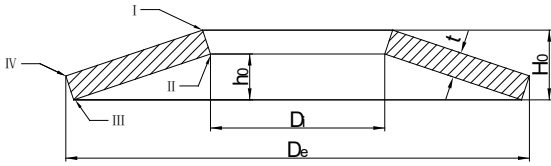


Fig. 2 Disc spring section diagram

Table 1. Standard and non-standard structural parameters

Category	D	d	H	t
Standard spring	140	72	11.2	8
Non-standard disk spring	138	98	10	7.5

The deformation and load values of a single disc spring often cannot meet the requirements of practical use, and it is necessary to use them in groups in actual applications. According to superposition to improve the bearing capacity, and to improve the deformation ability according to combination, the composite group combines both characteristics. The form of the combination of a single disc spring is shown in Table 2. The disc spring used in combination has the advantages of certain energy consumption capacity, and is commonly used in energy consumption and shock absorption [8].

Table 2. Combination diagram

Combination Form	Combination illustration
Single disc spring	
Double-stack disc spring	
clutch disc spring	
Composite combination disk spring	

3. Simulation analysis

(1) Tool Technical Specifications

Under the influence of periodic pulses, the hydraulic oscillator will produce axial vibrations with a frequency of 16Hz-17Hz and an amplitude of 3mm~10mm. The schematic diagram of its structure is shown in Figure 3 and the relevant technical parameters are detailed in Table 3.

Table 3. Technical parameter

Technical specifications	Value
working pressure difference, MPa	4~5
working pressure difference, Hz	16~17
axial force, KN	60~80
work hours, h	120
Vibration displacement, mm	3~10

(2) model construction

In actual working conditions, the disc spring assembly is located between the upper and lower washers. When

performing large deformation elastoplastic finite element analysis on the disc spring, the lower washer is completely restricted in degree of freedom, and the load is applied by the upper washer.

Material properties: The disc spring material is spring steel 60Si2MnA, with an elastic modulus of $E = 206\text{MPa}$, a Poissons ratio of $\mu = 0.3$, and a yield strength of 1300MPa. The stress-strain curve of the material is shown in Figure 3.

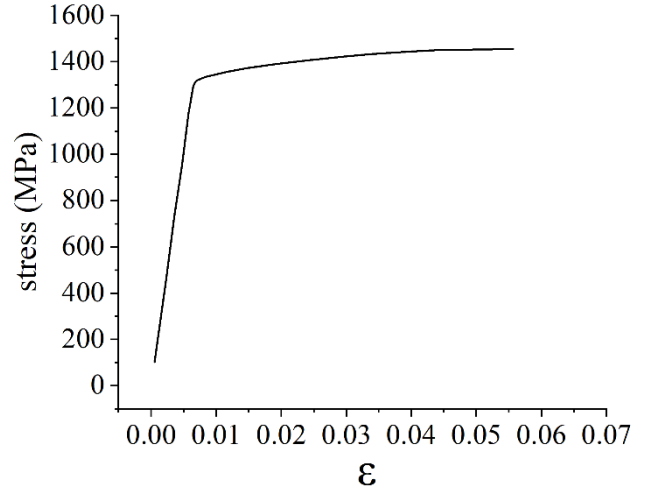


Fig. 3 Stress-strain curve

Grid partition: The top and bottom pads are used for coarse partitioning. During the loading process, the rigid disc spring is treated as a deformable body, and its grid is shown in Figure 4.

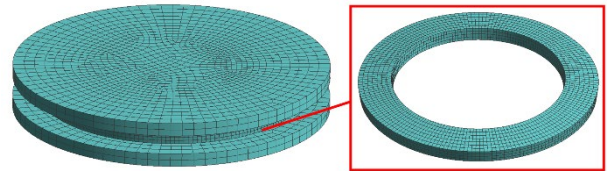


Fig. 4 Disc spring and upper and lower gasket grid diagram

Contact condition: The first contact pair consists of an upper washer and the supporting surface and conical surface of the disc spring. The second contact pair consists of a lower washer and the supporting surface and conical surface of the disc spring. The contact is defined as surface-to-surface contact, with a friction coefficient of 0.3. The penalty function defined by the friction coefficient is used for control.

Boundary condition: The lower washer is set to have a fixed constraint, limiting the axial upward degrees of freedom of the supporting surface of the disc spring. The loading condition is applied by the upper washer.

(3) Mechanical performance analysis

After applying a load of 80KN to the disc spring, the stress and deformation of the disc spring are shown in Figure 5 and Figure 6. From Figure 5, it can be seen that the stress near point I is the highest, with a maximum value of 1020MPa, which does not exceed the yield strength of the disc spring. The stress is uniformly distributed radially. From Figure 6, it can be seen that during the compression process, the lower supporting surface expands outward and the upper supporting surface caves inward. When the load is 80KN, the maximum deformation of the disc spring is 2.458mm, which is close to being flattened. From Figure 7, it can be seen that as the load on the disc spring increases, its displacement increases

linearly. In the stage close to flattening, the stiffness of the disc spring increases sharply, which is significantly different from the expected displacement increase and is not conducive to controlling the overall amplitude of the disc spring assembly. The overlay combination can improve the overall load-bearing capacity, but excessive overlay can lead to uneven loading in the combination, affecting the transmission efficiency of drilling pressure. The contact properties of the overlapped combination are face-to-face contact, and the ability to absorb and dissipate frictional energy is particularly evident. In contrast, the contact properties of the overlapped combination are line-to-line contact, with less frictional energy dissipation. Therefore, the overlapped combination is the optimal way, and the high thickness ratio h_0/t is the key parameter determining the mechanical performance of the small diameter ratio disc spring. The existing disc spring structure needs to be optimized to improve the mechanical performance of the single disc spring.

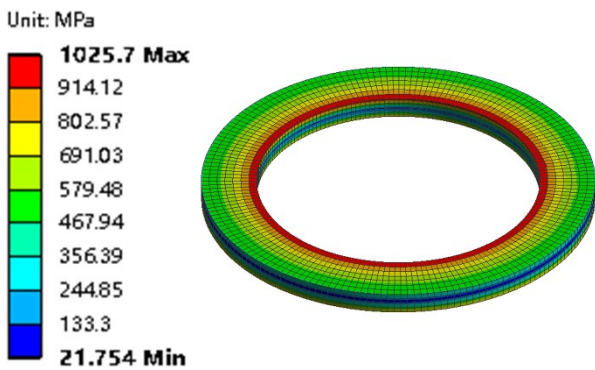


Fig. 5 Von Mises stress nephogram of disc spring under 80KN

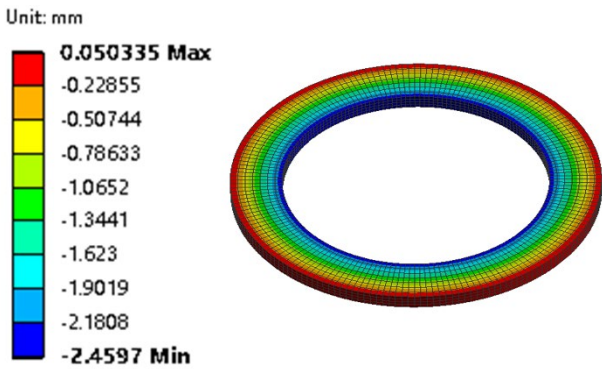


Fig. 6 80KN disc spring deformation nephogram

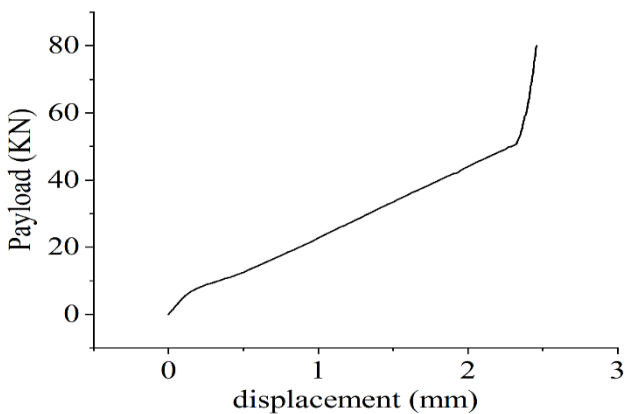


Fig. 7 Loading-displacement curve

(4) Fatigue analysis

Considering that the average stress has a significant impact on the fatigue life of disc springs[12], the Goodman

correction is used to modify the disc spring.

$$\sigma_a = \sigma_{-1} \left(1 - \frac{\sigma_m}{\sigma_b}\right), \quad (1)$$

In equation (1): σ_a is the fatigue limit amplitude; σ_{-1} is the fatigue limit under fully reversed cyclic loading; σ_m is the fatigue limit under symmetric cyclic loading; σ_b is the tensile strength.

When conducting fatigue life analysis on a disc spring, the fatigue life curve for 60Si2MnA is shown in Figure 8. After stress correction, fatigue life analysis was carried out on the disc spring. The fatigue life cloud diagram of the disc spring under symmetric cycling is shown in Figure 9.

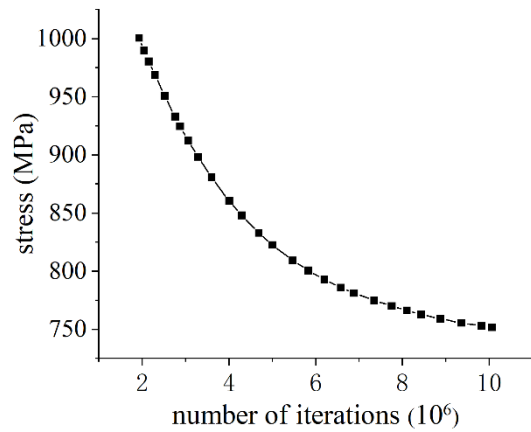


Fig. 8 S-n curve

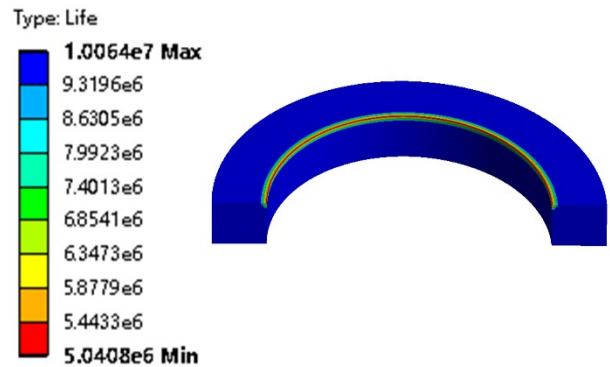


Fig.9 Disc spring life cloud diagram

The minimum lifespan of the disc spring is at point I, which experiences fatigue failure after 5,040,800 cycles (77h), which does not meet the required 120h. Therefore, it is necessary to optimize the design of the disc spring to increase its lifespan. One way to improve the lifespan of the disc spring is by increasing its thickness (t) to increase its rigidity [13].

4. Structural optimization

(1) Structural parameter optimization analysis

The national standard algorithm is a general algorithm for the universal characteristics of disc springs, proposed by J. O. ALMEN et al. in 1936[14,15]. This method is based on the S. TIMOSHENKO bending beam assumption and satisfies three basic assumptions during the solving process.

The cross-sectional area does not deform when subjected to load.

The material is an isotropic linear elastic substance. The influence of frictional forces between contact surfaces is neglected.

According to GB/T1972-2005:

$$F = \frac{4E}{1-\mu^2} \cdot \frac{t^4}{K_1 D^2} \cdot K_4^2 \cdot \frac{f}{t} \cdot [K_4^2 \cdot (\frac{h_0}{t} - \frac{f}{t})(\frac{h_0}{t} - \frac{f}{2t}) + 1] \quad (2)$$

In equation (1): p is the payload, N; E is the elastic modulus, MPa; μ is the Poissons ratio; t is the thickness of the disk spring, mm; f is the deflection of a single disk, mm; K is the calculation coefficient; Fz is the combined load on multiple disks, N; n is the number of disks in the stack.

The calculation coefficient is:

$$C = \frac{D}{d} \quad (3)$$

$$K_1 = \frac{1}{\pi} \times \frac{(\frac{C-1}{C})^2}{C+1} \times \frac{2}{C-1 \ln C} \quad (4)$$

$$K_2 = \frac{6}{\pi} \times \frac{\frac{C-1}{\ln C} - 1}{\ln C} \quad (5)$$

$$K_3 = \frac{3}{\pi} \times \frac{C-1}{\ln C} \quad (6)$$

$$K_4 = \sqrt{-\frac{C_1}{2} + \sqrt{(\frac{C_1}{2})^2 + C_2}} \quad (7)$$

According to formula (2), it can be seen that as the deformation increases, the load borne by the disk spring increases continuously. When the displacement amount $f=h_0$, the disk spring is flattened, and the load at this time is independent of the deformation amount, but is determined by the thickness t, which determines the ultimate load of the disk spring. Under the condition that the diameter ratio is determined, in order to improve the performance of the disk spring, the internal cone height h0 and thickness t of the disk spring are taken as design variables for optimization.

(2) parameter optimization

By establishing a parameterized model and combining the characteristics curve of the disc spring, when $h_0/t < 0.5$, the load and displacement vary linearly. The surface response method is used to optimize the parameters of the disc spring, with parameter ranges shown in Table 4.

Table 4. Parameter initial value and optimization range

Design parameters	Initial Value	Parameter Optimization Range
t/mm	7.5	7.5~12.1
h0/mm	2.5	2.0~2.5

The experiment was designed using the middle composite material design method with the maximum equivalent stress, minimum life and directional deformation of the disc spring as the optimization objectives. Nine test points were selected using this method, and the corresponding data is shown in Table 5.

After obtaining the experimental data, it is necessary to select the response model of the variables. Kriging model is a method for optimal linear unbiased estimation of unknown sample points[16]. In this paper, Kriging response surface model is used for response surface analysis of the structure. The response surface maps of the maximum equivalent stress orientation deformation and the minimum life quantity of the diaphragm spring are shown in Figure 10, Figure 11, and

Figure 12, respectively.

Table 5. Test data

Number	H0	t	Maximum stress, MPa	Directed deformation, mm	Minimum fatigue life, 106
1	2.35	9.8	870	1.5854	10.064
2	2.2	9.8	864.94	1.6011	10.064
3	2.5	9.8	874.35	1.5689	10.064
4	2.35	7.5	949.55	2.3254	8.8938
5	2.35	12.1	555.76	0.8080	10.064
6	2.2	7.5	888.78	2.1866	10.064
7	2.5	7.5	1026.2	2.4597	5.0408
8	2.2	12.1	554.79	0.8175	10.064
9	2.5	12.1	556.53	0.7985	10.064

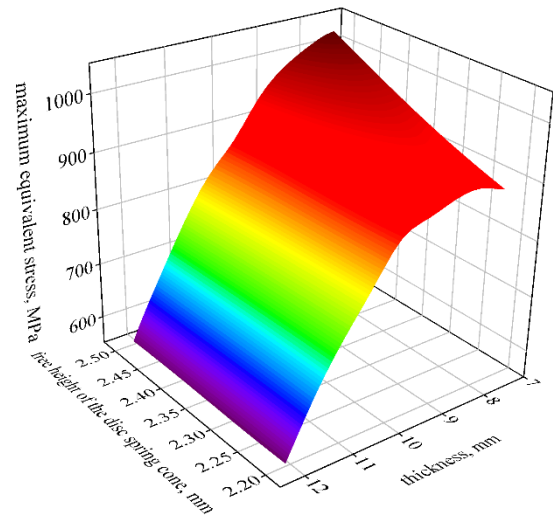


Fig. 10 Maximum equivalent stress response surface

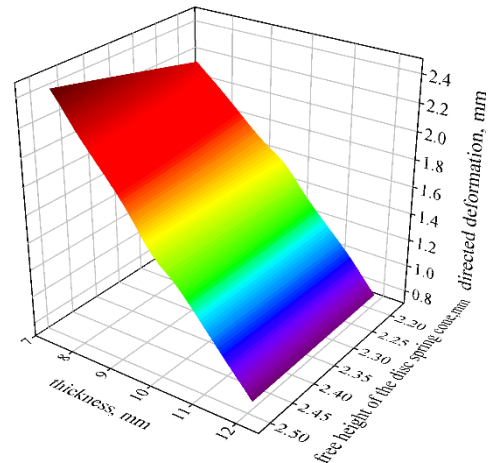


Fig. 11 Directional deformation response surface

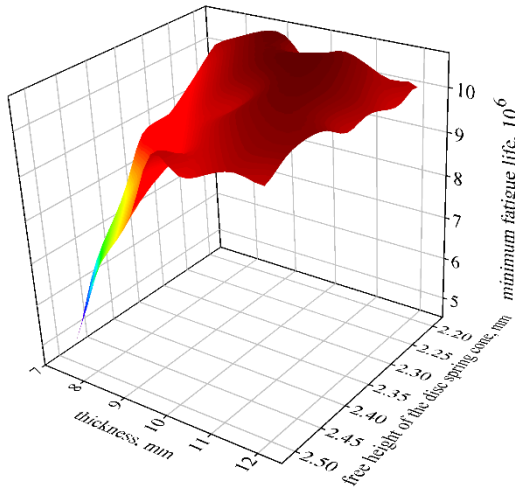


Fig. 12 Minimum life response surface

According to Figure 10, the maximum equivalent stress of a disc spring with a smaller diameter ratio gradually decreases with the increase of the spring thickness t . According to Figure 11, the selective deformation decreases with the increase of thickness and the decrease of inner cone height. According to Figure 12, the lifespan of the disc spring increases with the increase of thickness.

Taking into account the three objectives of maximum equivalent stress, directional deformation, and minimum service life, the parameters were optimized using a multi-objective genetic algorithm, resulting in three optimal solutions as shown in Table 6.

Table 6. Optimization scheme

solution	H0	t	maximum stress, MPa	directed deformation, mm	minimum fatigue life, 10 ⁶
1	2.35	9.8	870	1.5854	10.064
2	2.2	9.8	864.94	1.6011	10.064
3	2.5	9.8	874.35	1.5689	10.064

According to the data in Table 6, in the multi-objective optimization with the objectives of maximum equivalent stress, directional deformation, and minimum life, the working stroke and life of scheme 3 are the best. Therefore, we choose scheme 3 as the final optimization result. After parameter adjustment, the thickness of the disc spring is 12.1 and the inner cone height is 2.3. The optimized stress, deformation, and life cloud maps of the disc spring are obtained by re-simulating the results after optimization, as shown in Figures 13, 14, and 15, respectively.

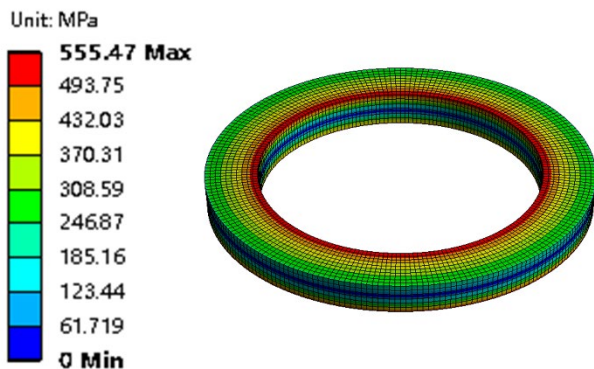


Fig.13 The optimized stress cloud diagram

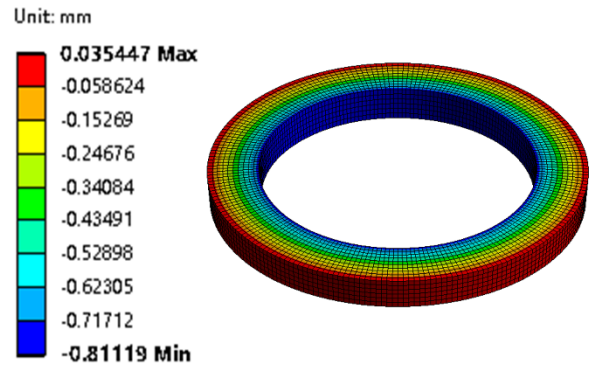


Fig.14 Optimized deformation cloud diagram

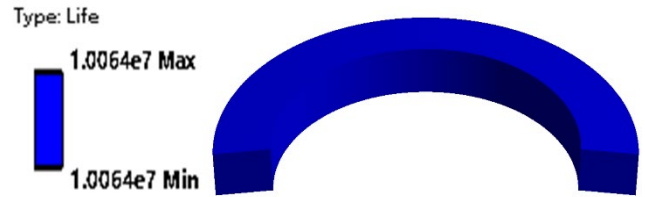


Fig.15 Optimized life cloud diagram

compare the performance before and after optimization, the results are shown in Table 7.

Table 7. Performance of disc spring before and after optimization

Disc spring	Maximum stress, MPa	Directed deformation, mm	Minimum fatigue life, 10 ⁶
Pre-optimisation	1026.2	2.4597	5.0408
Optimised	555.47	0.8111	10.064

According to Table 7, the maximum equivalent stress of the optimized disc spring decreased by 45.9%, the minimum fatigue life reached 154 hours, and the directed deformation accounted for 35.8% of the working stroke. The load-displacement curves of the disc spring before and after optimization are shown in Figure 16, which indicates that increasing the thickness improves the stiffness of the disc spring. Based on the response surface models for stress, deformation, and life of the disc spring, the primary geometric factor affecting the performance is thickness, while the internal cone height affects the working stroke. The optimized disc spring, shown in Figure 17, achieved the expected goals when applied to the 172-type hydraulic oscillator.

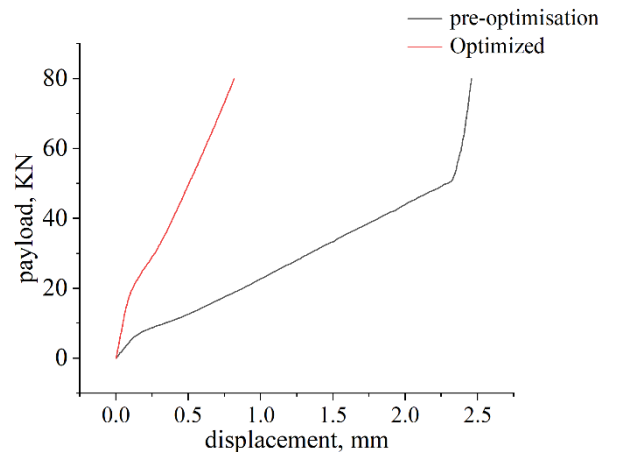


Fig. 16 Load displacement curve before and after optimization



Fig. 17 Optimized disc spring

5. Conclusions

A response surface model was established with the maximum equivalent stress, directional deformation, and minimum lifespan as objectives and the thickness and inner cone height of the disc spring as design variables. After application, the expected goals were achieved.

The first geometric elements affecting the disc springs mechanical performance were determined using the response surface method to be thickness and inner cone height, which affect the working stroke of the disc spring.

By using the national standard algorithm, the optimization direction of the disc spring was determined. After parameter optimization, the optimal structural parameters were obtained: a thickness of 12.1, an inner cone height of 2.3. The maximum stress was reduced by 35.8%, the directed deformation accounted for 35.8% of the working stroke, and the minimum lifespan reached 154 hours. In the development of contemporary embroidery art, traditional embroidery is made by hand, so the overall production quality has been greatly guaranteed. However, because of labor, the cost is higher and the efficiency is slower. Facing the contemporary fashion design needs, mass production cannot be carried out. Therefore, it is necessary to meet the needs of consumers, properly carry out industrialization treatment, and make the development of the whole embroidery art serve the marketization, thus providing help for the promotion of artistic influence. For relevant personnel, let hand embroidery and modern industry be effectively combined. By using intelligent modern manufacturing technology instead of traditional manual methods, embroidery art can develop sustainably. New technologies and processes can improve the quality of embroidery production. Moreover, through the new technology, under the requirements of high standards, it can not only preserve the original aesthetic feeling, but also satisfy peoples love for free art. Therefore [1], when designing clothing, it is necessary to consider whether the machinery and equipment can be produced, print and dye the pattern in the clothing, and form a hollow design, which can further enhance the aesthetic feeling of the whole design. However, fashion designers should not rely too much on machines and equipment, and still focus on traditional techniques. In the embodiment of all artistic values, combined with the designers own ideas, let the traditional embroidery art and modern fashion design coordinate with each other,

form a complementary effect, and let the modern fashion art develop in the long run.

References

- [1] YINAO SU, XIURONG DOU, JIAJIN WANG. Antifriction Tool and Its Application[J]. Oil Drilling & Production Technology, 2005,27(2): 78-80.
- [2] CHEN C W, ZHOU Y C, SHEN R C, et al. Overview of Drag Reducing Technologies in Coiled Tubing Drilling[J]. PETROLEUM DRILLING TECHNIQUES, 2010,38(1): 29-31.
- [3] SHI H Z, CHENG P F, MU Z J, et al. Development and application of pin type hydraulic oscillator[J]. China Petroleum Machinery, 2021,49(11): 17-23.
- [4] RUIQING MING, SHIZHONG ZHANG, HAITAO WANG, et al. Research Status and Prospect of Hydraulic Oscillator Worldwide[J]. PETROLEUM DRILLING TECHNIQUES, 2015,43(5): 116-122.
- [5] KONG LING RONG, WANG YU, ZOU JUN, et al. Development status and prospect of hydro-oscillation drag reduction drilling technology[J]. Oil Drilling & Production Technology, 2019,41(01): 23-30.
- [6] LIU Y, CHEN P, WANG X, et al. Modeling friction-reducing performance of an axial oscillation tool using dynamic friction model[J]. Journal of Natural Gas Science and Engineering, 2016,33: 397-404.
- [7] ZHU XIAO HUA, LIU SHAO HU, JING JUN, et al. Research on the Mechanical Property of Non-standard Disc Spring for Drilling Tools[J]. China Petroleum Machinery, 2012,40(6): 22-25.
- [8] CHANG HAI LIN. STUDY ON MECHANICAL PERFORMANCE AND APPLICABILITY OF THREE-DIMENSIONAL ISOLATION BEARING[D]. BEIJING UNIVERSITY OF TECHNOLOGY, 2020.
- [9] XIAO FA PING. Design of New Type Three-dimensional Seismic Isolation Device and Application Study in Ancient Timber Structure[D]. Guangzhou University, 2018.
- [10] HUAN WU. Research on disc spring isolation device[D]. Yangzhou University, 2012.
- [11] XIAOSONG WEN, GONGHUI LIU, YANG WANG, et al. Optimal Design and Mechanical Properties of Non-Standard Belleville Spring for Oil Drilling[J]. China Petroleum Machinery, 2020,48(6): 9-17.
- [12] YUAN ZHANG, KUNPENG HE, MANSHAN ZHOU, et al. Fatigue Life Analysis of Disc Springs of Disc Brakes[J]. Coal Mine Machinery, 2019,40(5): 75-78.
- [13] CHUIZONG HUANG, MAIXIANG CUI. Structure Optimization of Wet Brake of Explosion-Proof Rubber Wheel Car in Underground Coal Mine[J]. Lubrication Engineering, 2022,47(11): 69-74.
- [14] Almen J O, LASZLO A. The Uniform-Section Disk Spring[J]. Trans. ASME, 1936,58: 305-314.
- [15] National Spring Standardization Technical Committee, Disc spring standard :GB/T1972—2005 [S], Beijing: China Standard Press, 2005.
- [16] HUIMIN XUE, KAIXI ZHAO, XIAOLI J. I. Structural Design and Optimization of Fixed Plate Pressure Plate of New Ball Lapping Machine[J]. Machine Tool & Hydraulics, 2022,50(15): 87-91.